Ion selectivity and gating of small conductance Ca^{2+}-activated K^+ channels in cultured rat adrenal chromaffin cells

YoungBae Park

Department of Physiology and Biophysics, SJ-40, University of Washington, School of Medicine, Seattle, WA 98195, USA

1. The ion selectivity and gating of apamin-sensitive, small conductance Ca^{2+}-activated K^+ (SK) channels were studied in cultured rat adrenal chromaffin cells using patch clamp techniques.

2. The amplitude of slow tail currents showed a bell-shaped dependence on depolarization potentials. Slow tail currents were abolished in a Ca^{2+}-free external solution or by adding 100 μM Cd^{2+} to the external solution. Reversal potentials followed the predictions of the Nernst equation for a K^+ electrode.

3. Slow tail currents were largely blocked by external application of apamin (dissociation constant, K_d, 4·4 nM), (+)-tubocurarine (K_d, 20 μM), and tetraethylammonium (K_d, 5·4 mM).

4. The relative permeability (P_X/P_K, where X may be any one of the ions listed) of SK channels was: Tl^+ (1·87) > K^+ (1·0) > Rb^+ (0·81) > Cs^+ (0·16) > NH_4^+ (0·11). Na^+, Li^+ and methylamine were not measurably permeant ($P_X/P_K < 0·005$). Open SK channels seem to have an effective pore diameter of 0·34–0·38 nm. The relative conductance (g_X/g_K) was: Tl^+ (1·29) > K^+ (1·0) > Rb^+ (0·85) > Cs^+ (0·45) ≈ NH_4^+ (0·44).

5. With mixtures of Tl^+ and K^+, SK channels showed anomalous mole-fraction behaviour.

6. Ca^{2+} dependence of SK channel gating was studied using inside-out macropatches. The $[Ca^{2+}]$ required for half-maximal activation and the Hill coefficient were 0·69 μM and 1·7, respectively, and independent of membrane potentials.

7. Single-channel conductance was 13–14 pS (160 mM K^+).

Calcium ions are an important intracellular messenger controlling many cellular functions. Among these Ca^{2+}-controlled processes, Ca^{2+}-activated K^+ channels ($I_{K(Ca)}$) play essential roles in regulating cellular functions by coupling intracellular Ca^{2+} levels and membrane potential to K^+ efflux (Blatz & Magleby, 1987; Latorre, Oberhauser, Labarca & Alvarez, 1989; Hille, 1992). It has been known for a long time that intracellular Ca^{2+} can control K^+ permeability of the cell membrane (Gárdos, 1958), but the prevalence and diversity of $I_{K(Ca)}$ channels were underestimated until the advent of the patch clamp technique. Since the first demonstration of large-conductance $I_{K(Ca)}$ channels (BK) in cultured bovine chromaffin cells (Marty, 1981), $I_{K(Ca)}$ channels have been observed in most tissues and subsequent studies showed they are quite heterogeneous. Channel conductances range from a few to several hundred picosiemens and Ca^{2+} sensitivity, voltage dependence and pharmacological properties vary among different subtypes (Blatz & Magleby, 1987; Latorre *et al.* 1989). $I_{K(Ca)}$ channels are loosely classified into large-conductance, intermediate-conductance and small-conductance families (Blatz & Magleby, 1987; Latorre *et al.* 1989). The gating of BK channels is both Ca^{2+} and voltage dependent and most BK channels are blocked by charybdotoxin. Due to their long open times, large unitary currents and prominence in most excitable cells, BK channels have been studied extensively (Blatz & Magleby, 1987; Latorre *et al.* 1989).

In contrast, small-conductance $I_{K(Ca)}$ channels (SK), which are selectively blocked by apamin, are more sensitive to $[Ca^{2+}]_i$ and have a small unitary conductance of 4–20 pS, were recognized more recently (Blatz & Magleby, 1986; Lang & Ritchie, 1990). Due to a higher Ca^{2+} sensitivity at the resting potential, SK channels are important in controlling the interspike interval by producing long hyperpolarizing pauses after action potentials (after-hyperpolarization) and spike frequency adaptation during depolarizing influences (Yarom, Sugimori & Llinás, 1985; Lang & Ritchie, 1990). For example, periodic opening of apamin-sensitive SK channels, which is associated with the oscillation of $[Ca^{2+}]_i$ following stimulation of gonadotrophin-releasing hormone, modulates electrical activity of pituitary gonadotrophs (Tse & Hille,

1992). Despite their functional importance, the biophysical properties of SK channels have not been well characterized, perhaps because of the difficulty in isolating SK currents from other currents. A recent report of prominent SK currents in rat adrenal chromaffin cells (Neely & Lingle, 1992*a*) has allowed the study of the biophysics of SK channels in detail.

Here, the ion selectivity and the Ca^{2+} and voltage dependence of gating of apamin-sensitive SK channels of cultured rat adrenal chromaffin cells are characterized. Part of this work has appeared previously in abstract form (Park & Hille, 1993).

METHODS

Solutions

The composition of normal Tyrode solution was (mM): NaCl, 150; KCl, 2·5; $CaCl_2$, 10; $MgCl_2$, 1; Hepes, 10; and glucose, 5; adjusted to pH 7·40 with NaOH. When high $[K^+]_o$ was used, an equimolar amount of NaCl was omitted. For selectivity measurements, solutions containing 30 mM test cations were based on *N*-methyl-D-glucamine (NMG) titrated with methanesulphonic acid (MSA) (mM): NMG, 120; MSA, 120; XCl, 30 (where X may be one of the following: Li^+, Na^+, K^+, Rb^+, Cs^+ or NH_4^+); $CaCl_2$, 10; Hepes, 10; and glucose, 5; adjusted to pH 7·40 with NMG. For solutions containing Tl^+ ions, nitrate salts were used instead of chloride salts and reversal potentials were compared with those measured with KNO_3.

Small conductance $I_{K(Ca)}$ channels were activated by Ca^{2+} entry through voltage-activated Ca^{2+} channels, so the internal solution for whole-cell recording was designed to optimize Ca^{2+} currents during depolarization as well as to isolate SK currents as slow tail currents following the depolarization. It consisted of (mM): potassium aspartate, 120; KCl, 20; $MgCl_2$, 5; K_2ATP, 3; Na_3GTP, 0·1; leupeptin, 0·1; EGTA, 0·1; and Hepes, 20; adjusted to pH 7·20 with KOH. Total $[K^+]_i$ was 162 mM. SK currents were stable for up to 1 h.

For inside-out patch recordings, the pipette solution contained (mM): potassium aspartate, 160; $CaCl_2$, 2; and Hepes, 10; adjusted to pH 7·40 with NMG. The superfusion solution contained (mM): potassium aspartate, 160; EGTA, 2; Tris-ATP, 2; and Hepes, 10; adjusted to pH 7·20 with NMG at 22–24 °C. ATP was included to suppress ATP-sensitive K^+ channels (unpublished data). Varying amounts of $CaCl_2$ were added to this solution to yield appropriate values of free Ca^{2+} between 17 nM and 2 μM. Stability constants used in the calculation of free Ca^{2+} (pH 7·2) were $10^{3·8}$ M^{-1} for binding of Ca^{2+} by ATP, and $10^{6·8}$ M^{-1} for binding by EGTA (Martell & Smith, 1974). For 4·3 and 11 μM Ca^{2+} solution, EGTA was omitted and 46 and 118 μM of $CaCl_2$ was added, respectively. Modified Hanks' solution, which was used for dissociation of chromaffin cells, contained (mM): NaCl, 110; KCl, 5·4; $NaHCO_3$, 23·8; NaH_2PO_4, 10; Hepes, 20; glucose, 10; penicillin G, 250 U ml^{-1}; and streptomycin, 250 μg ml^{-1}; adjusted to pH 7·40 with NaOH.

In whole-cell recording, tetrodotoxin (200–500 nM) was added to the bath solution to block current flow through Na^+ channels. Apamin, (+)-tubocurarine, NMG, MSA and EGTA (97% purity) were obtained from Sigma Chemical Co. (USA), CsCl from BRL (Gaithersburg, MD, USA; ultrapure grade), ATP and GTP from Pharmacia LKB (Alameda, CA, USA) and tetrodotoxin and leupeptin from Calbiochem Corp. (La Jolla, CA, USA). All experiments were performed at room temperature (22–24 °C) and experimental values are reported as means ± S.E.M.

Isolation and culture of rat adrenal chromaffin cells

Experiments were made on primary cultures of chromaffin cells from rat adrenal glands, prepared as described by Neely & Lingle (1992*a*) with slight modification. Briefly, a 250–300 g male rat was killed by excessive inhalation of the anaesthetic methoxyflurane. The adrenal medullas were first treated for 30–40 min at 37 °C using modified Hanks' solution (1 ml), containing: collagenase type I (Sigma, USA), 3·0 mg ml^{-1}; hyaluronidase type I-S (Sigma), 2·4 mg ml^{-1}; and DNase type I (Sigma), 0·2 mg ml^{-1}; and further digested for 10 min after the addition of an equal volume of modified Hanks' solution containing trypsin type XIII (Sigma) at 1 mg ml^{-1}. After washing twice by centrifugation, the pelleted cells were resuspended in 0·5–1 ml Dulbecco's modified Eagle's medium (DMEM; Gibco, USA) supplemented with horse serum (7·5%), fetal calf serum (2·5%) and antibiotics, then plated on a coverglass (18 mm square, No. 1, Corning, USA) coated with collagen (Vitrogen-100; Celtrix, Santa Clara, CA, USA) and maintained in a 10% CO_2–90% air, water-saturated incubator at 37 °C for up to 7 days. Cells were used starting 1 day after dissociation because SK currents were absent or small during the first day of culture.

Electrophysiological recording

Whole-cell and inside-out patch clamp methods (Hamill, Marty, Neher, Sakmann & Sigworth, 1981) were used to control membrane potential and measure transmembrane currents with an Axopatch 1-B patch clamp amplifier (Axon Instruments, Inc., Foster City, CA, USA). Pipettes were pulled from glass haematocrit tubes (75 μl purple glass; VWR, Seattle, WA, USA), Sylgard-coated for inside-out patch recording with resistances of 1·5–3 MΩ. Cell membrane capacitance of 3–14 pF (7·2 ± 2·3 pF, $n = 33$) was compensated and usually series-resistance compensation was not used because SK currents were small (usually 200–400 pA). Whole-cell currents were low-pass filtered at 1 kHz (−3 dB, 4-pole Bessel) and digitized with the BASIC-FASTLAB System (Indec Systems Inc., Sunnyvale, CA, USA) and stored on an IBM AT computer. In whole-cell recording, only the holding current before the depolarization and the slow tail current following repolarization are shown in the figures. For reversal potential measurement, leak current was corrected by subtracting current responses to rapid-step voltage pulses without the preceding conditioning depolarization and zero-current levels are marked as dashed lines.

Inside-out macropatches containing a large area of the cell membrane were obtained by forming gigaseals rather slowly over 1–2 min with Sylgard-coated glass pipettes. Sylgard coating close to the tip of a patch pipette retarded the establishment of the gigaseal and resulted in the formation of a large, Ω-shaped membrane patch inside the pipette. Thereafter, the pipette was withdrawn slowly from the coverglass, which either lifted the whole cell or resulted in the formation of a membrane vesicle at the tip. Touching the tip onto a nearby Sylgard plate resulted in the disintegration of the exposed area of the cell membrane, leaving the inside of

the membrane exposed to the bath solution. Application of a high-Ca^{2+} solution (11 μM) to such inside-out patches using the rapid perfusion system (see below) activated large inward currents (100–300 pA at −100 mV, see Fig. 7*A*) within a couple of seconds and the patches were stable for up to 40 min. Membrane potentials and currents of inside-out patches were filtered at 10 kHz and stored on a pulse code modulator data recorder (A. R. Vetter Co., Rebersburg, PA, USA). They were later digitized using the computer after refiltering at 100–1000 Hz.

Correction for liquid-junction potential

Junction potentials were measured against a ceramic-junction, saturated KCl reference electrode (model 29402, Beckman Instruments, Inc., Fullerton, CA, USA) by comparing the zero-current potential in symmetrical solution (potassium aspartate pipette solution both in the pipette and the bath) and after replacement of the bath solution with the solution used in the experiment. This potential amounted to 9 mV (pipette solution negative) if the pipette contained potassium aspartate solution and the bath contained normal Tyrode solution. All membrane potentials and reversal potential measurements reported in this paper were corrected accordingly. A salt bridge (2% agar in 150 mM NaCl) was used as the bath reference electrode in experiments and its junction potential was corrected in a similar way.

Measurement of ion selectivity

Reversal potentials were measured under bi-ionic conditions by determining the potential at which membrane current was zero. The permeability of test ion X^+ relative to K^+ (P_X/P_K) was calculated from the shift of the reversal potential (E_r) upon exchanging the 30 mM K^+ solution, which contained no other monovalent, permeant cations, with an identical solution except that the K^+ was replaced by a test cation, X^+:

$$\Delta E_r = E_{r,X} - E_{r,K} = (RT/F)\ln(P_X[X^+]_o/P_K[K^+]_o), \quad (1)$$

where R, T and F have their usual thermodynamic meanings.

Fluctuation analysis of macropatch current

The apparent single-channel conductance of macropatch current was estimated using stationary fluctuation analysis (Sigworth, 1980), assuming that macropatch channels activated by application of intracellular Ca^{2+} are identical and independent channels. After reaching steady-state current levels by superfusion of Ca^{2+} solutions, current variances of 1 s current segments were analysed after filtering with a four-pole Bessel filter set to 100 Hz and sampling at 10 ms intervals, then plotted against mean current levels after subtraction of background variance and leak current. A parabola of the form $\sigma_I^2 = iI - I^2/N$ was fitted to the data, where σ_I^2 is the current variance, i the unitary current, I the mean current and N the total number of channels in the macropatch.

Perfusion systems

Two perfusion methods were used to change experimental solutions. Bath perfusion by gravity was used when rapid solution change was not necessary and it took ~30 s to completely exchange the solution of the ~100 μl experimental chamber made of Sylgard. For rapid solution exchange, a glass pipette with a tip diameter of 50–100 μm within which seven polyethylene tubes (PE-10; i.d. 0·28 mm, o.d. 0·61 mm) were packed as close to the tip as possible (~1 mm) which was placed 100–200 μm from the cell or membrane patch (Neely & Lingle, 1992*a*). When the perfusion tip was placed properly, solution exchange was complete within < 200 ms as determined by measuring holding current changes. Solution flow was switched by computer-controlled solenoid valves.

RESULTS

The main goal of this study was to investigate the ion selectivity and gating of SK channels. Currents through SK channels were isolated both as slow tail currents in whole-cell recording conditions to examine ion selectivity, and as macropatch currents in inside-out patch recording to determine the Ca^{2+} and voltage sensitivity of SK channel gating.

Ca^{2+} dependence of slow tail currents

Identification of $I_{K(Ca)}$ channels requires a demonstration that the channels are activated by elevation of intracellular Ca^{2+} and are selective for K^+ ions. The Ca^{2+} dependence of slow tail currents was studied in whole-cell recording conditions using elevated K^+ (30 mM) and 10 mM Ca^{2+} in the bath and a pipette solution containing 162 mM K^+. Figure 1*A* shows slow, inward tail currents at a holding potential of −60 mV after 1 s depolarizations. The membrane potential was stepped to potentials between −40 and +70 mV. Slow tail current was barely activated following the conditioning voltage step to −40 mV. Following the step to −20 mV, a large inward tail current was activated that decayed with a half-decay time ($t_{1/2}$) of 1·02 s, and after the step to 0 mV the tail current became still larger and slower ($t_{1/2}$ = 2·01 s). With conditioning voltage steps to more positive potentials, the tail current amplitude became smaller and the decay time course faster, so with +60 mV, it was tiny and decayed with a $t_{1/2}$ of 0·20 s. Thus, the amplitude and time course of slow tail currents following depolarization depended on the conditioning depolarization potentials.

The current–voltage relation (Fig. 1*B*) shows the dependence of slow tail current amplitude on the conditioning potential more clearly. Current amplitudes were measured 220–230 ms following repolarization to avoid possible contamination of tail currents by BK currents (Neely & Lingle, 1992*a*; Solaro & Lingle, 1992) and plotted against the conditioning potentials (●). As shown in Fig. 1*A*, activation of the tail currents required depolarizations positive to −30 mV, reached a peak in the voltage range −10 to +10 mV and decreased again with higher depolarizations. A plot of the time integral of slow tail current (■) showed a similar relationship, but had a sharp peak at 0 mV (Fig. 1*B*).

The bell-shaped current–voltage relation for the tail current suggests that the activation of the slow tails depends on Ca^{2+} entry during depolarizations. Indeed, in

the same cell, the large, inward tail current recorded at −80 mV was completely abolished by the addition of 100 μM Cd^{2+} to the bath solution or by the complete substitution of extracellular Ca^{2+} with equimolar Mg^{2+} (Fig. 1*C*). The current–voltage relation of Ca^{2+} currents during depolarization, recorded in another cell with solutions designed to block K^+ currents, is shown in Fig. 1*D*. It is similar to the voltage dependence of integrated tail currents in Fig. 1*B*, which has been scaled and superimposed as a dashed line in Fig. 1*D*. A plot of half-decay times of slow tail currents *versus* voltage had a shape very similar to the plot of integrated currents in Fig. 1*D* (data not shown).

As the duration of the conditioning step was increased, both the amplitude and half-decay time of the tail current increased. Figure 2*A* shows inward tail currents during repolarization to −80 mV after voltage steps to 0 mV ranging in duration from 0·1 to 1·5 s. All tail currents had a brief, initial decaying component (time constant (τ) ~ 5 ms), consistent with the time course of deactivation of BK

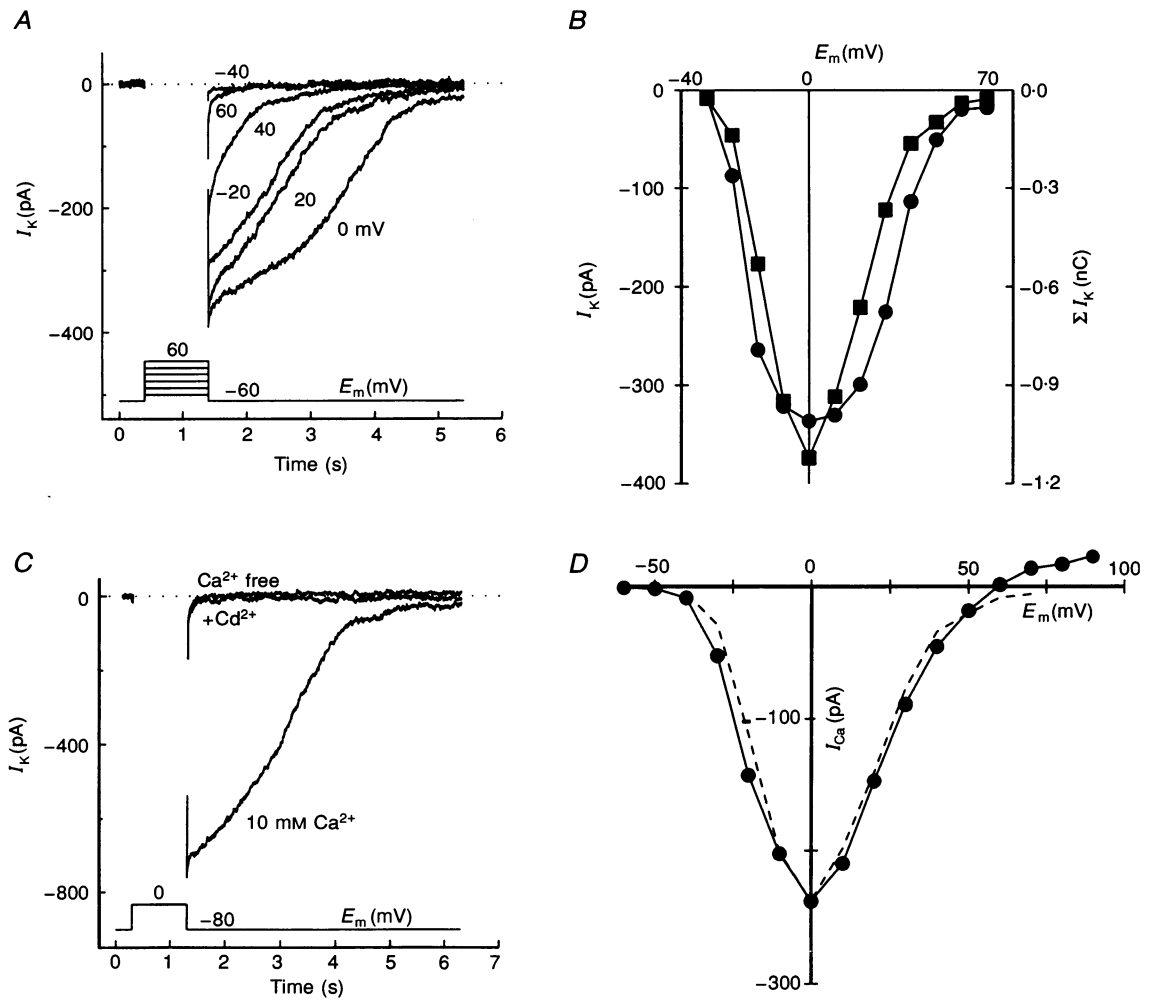

Figure 1. Ca^{2+} dependence of slow tail currents

A, slow tail currents were recorded at a holding potential of −60 mV following 1 s depolarization to −40 to +70 mV in 10 mV steps. In *A* and *C*, currents during the depolarization were not recorded and zero-current levels are indicated as dotted lines. $[K^+]_o$ was 30 mM in *A* and *C*. Series resistance, 2·6 MΩ; cell capacitance, 5·4 pF. *B*, plot of amplitude (●) of slow tail currents measured at 220–230 ms after depolarization and integral (■) of slow tail currents against depolarization potentials in the same cell. *C*, suppression of slow tail currents by the addition of 100 μM Cd^{2+} or the complete substitution of extracellular Ca^{2+} with equimolar Mg^{2+} (Ca^{2+} free). Holding potential, −80 mV; same cell as in *A*. *D*, current–voltage relation of Ca^{2+} currents (●), which were activated during depolarization and measured in another cell with Cs^+ in the pipette solution and 150 mM TEACl bath solution containing 10 mM Ca^{2+}. For comparison, integrals of slow tail current plotted in *B* are superimposed as a dashed line after scaling to the Ca^{2+} current amplitude at 0 mV.

channels in rat adrenal chromaffin cells (Neely & Lingle, 1992*a*). The 0·1 s depolarization elicited a small tail current, with a time course after the first 20 ms which can be described by two exponentials with τ values of 0·13 and 1·69 s (fast $\tau = 0{\cdot}17 \pm 0{\cdot}07$ s, $n = 6$; slow $\tau = 1{\cdot}30 \pm 0{\cdot}28$ s, $n = 4$). With longer test pulses ($\geqslant 0{\cdot}3$ s), tail currents followed a complex time course with a plateau. The later part (from ~2·5 s after repolarization) decayed exponentially with a time constant ($1{\cdot}39 \pm 0{\cdot}17$ s, $n = 9$) similar to that after the 0·1 s depolarization. In the experiment of Fig. 1*A*, a similar time course with two exponentials (fast and slow) was observed for slow tail currents elicited by 1 s depolarization to voltage ranges where the Ca^{2+} entry was small. For example, time constants of fast and slow decay were 0·13 and 1·12 s for the tail current activated by depolarization to +60 mV in Fig. 1*A*. In Fig. 2*B*, the amplitude (●) and half-decay time (□) of tail currents are plotted against the duration of the depolarization potentials. Both increased with the duration of depolarizations (< 0·5 s), but the current amplitude was almost saturated and half-decay time was already completely saturated at 0·5 s depolarization. A plot of the time integral of tail current against command duration had a shape similar to the current amplitude plot (data not shown). In four other cells, the saturation occurred at 0·5, 0·9, 1·1 and 1·7 s of depolarization, possibly reflecting variability in the size of Ca^{2+} currents.

K^+ selectivity of slow tail currents

To test if the Ca^{2+}-activated channels responsible for the slow tail currents were K^+ selective, reversal potentials were measured with different $[K^+]_o$. Reversal potentials were measured by applying a step-like series of 10 ms voltage pulses in 5–10 mV steps during the plateau period of the slow tail current elicited by a 1 s voltage step to 0 mV. Figure 3*A* shows the tail current recorded with 2·5 mM $[K^+]_o$ in response to two cycles of voltage steps ranging from −140 to −60 mV from a holding potential of −60 mV. The first step (●) is shown on an expanded time scale in Fig. 3*B*. The current–voltage plot (●) shows that the current reversed sign around −98 mV (Fig. 3*D*). The second cycle gave the same reversal potential and a smaller slope conductance. The step method of reversal potential measurement is much faster and gives the same value as the successive measurement of slow tail currents with different repolarization potentials (Fig. 3*C* and *D* (▲)).

The slow tail current was cation selective. With normal Tyrode solution containing 2·5 mM K^+ and 175 mM Cl^-, the reversal potential of $-100 \pm 2{\cdot}1$ mV ($n = 22$; Fig. 3*F*) was far from the Nernst potential for Cl^- (−45 mV), and when methanesulphonic acid (MSA) was substituted for extracellular Cl^-, there was no change in reversal potential (data not shown).

The current–voltage relations for four values of $[K^+]_o$ in one cell are shown in Fig. 3*E* and the averaged reversal potentials are plotted against $[K^+]_o$ in Fig. 3*F*. With 2·5 mM $[K^+]_o$ and 162 mM $[K^+]_i$, the current–voltage relation showed outward-going rectification (−41 pA at −140 mV, 103 pA at −60 mV; Fig. 3*D*), which could be described by the Goldman–Hodgkin–Katz current equation (Hille, 1992). It became more linear with higher $[K^+]_o$, and with 30 mM $[K^+]_o$ was nearly ohmic over the test potential range (Fig. 3*E*). The measured reversal potentials agree well with the predictions of the Nernst equation for a K^+ electrode (continuous line, Fig. 3*F*). Therefore, it is concluded that slow tail currents of rat

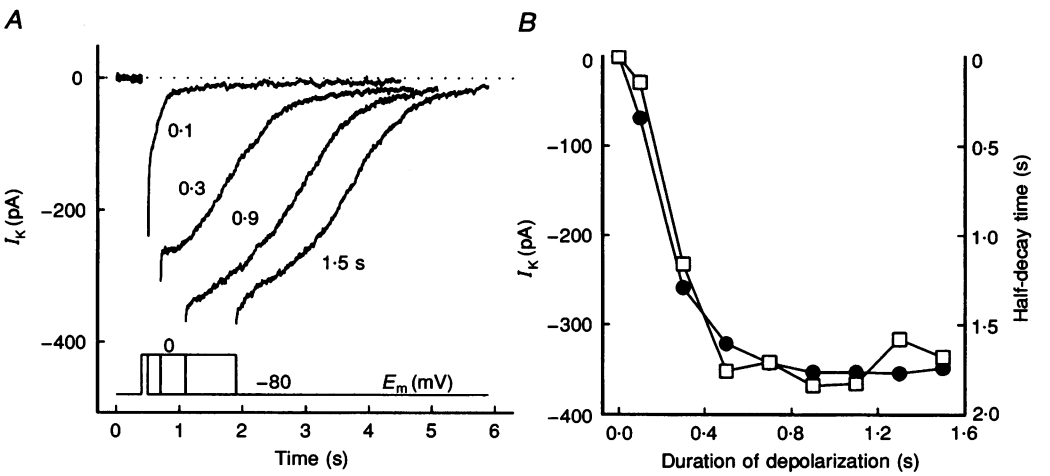

Figure 2. Cumulative effect of depolarization on slow tail currents

A, increase in amplitude and duration of slow tail currents with longer depolarizing pulses. $[K^+]_o$ was 30 mM. *B*, current amplitude (●), measured 150 ms following the repolarization, and half-decay time (□) of slow tail currents plotted against depolarization duration.

adrenal chromaffin cells at negative holding potentials following depolarization steps consist of K^+ currents through Ca^{2+}-activated K^+ channels.

Pharmacology of the Ca^{2+}-activated K^+ channels

This study of pharmacological properties of slow tail currents extends the results of Neely & Lingle (1992*a*) in a quantitative way and scrutinizes the component of current that has been reported to be insensitive to apamin and (+)-tubocurarine (dTC).

Apamin, an octadecapeptide from honey-bee venom, has been used as a specific blocker of SK channels in several preparations (Blatz & Magleby, 1987). External apamin reduced the slow tail currents of rat adrenal chromaffin cells (Fig. 4*A*). At −80 mV with 30 mM K^+ bath solution, 10 nM and 2 μM apamin reduced the inward tail current by 62 and 91%, respectively, in this cell and the mean reduction was 65 ± 9 ($n = 9$) and 92 ± 6% ($n = 10$), respectively; this corresponds to a K_d of 4·4 nM, assuming 1:1 binding between apamin and channel (Cook & Haylett, 1985; Seagar, Marqueze & Couraud, 1987) and a maximal block of 92%. Apamin (2 μM) blocked slow tail currents rapidly (< 10 s), but the wash-out was rather slow, recovering only 26% ($n = 2$; 30 and 23%) in 4 min after the wash-out of apamin, which would correspond to a time constant of ~800 s.

Like apamin, some diquaternary neuromuscular blocking agents, including dTC, reversibly block hyperpolarizing after-potentials or after-hyperpolarization currents, which are known to be due to activation of SK channels (Cook & Haylett, 1985; Goh & Pennefather, 1987). Figure 4*B* shows the dose–response relation of dTC block. At −80 mV with 30 mM K^+ bath solution, 2 mM dTC blocked 98% of slow tail current in this cell (Fig. 4*B*, inset). As with apamin, slow tail current was blocked incompletely by 2 mM dTC (92 ± 5%, $n = 15$). A Michaelis–Menten relationship (continuous line) fitted to the results suggests that 92·7%

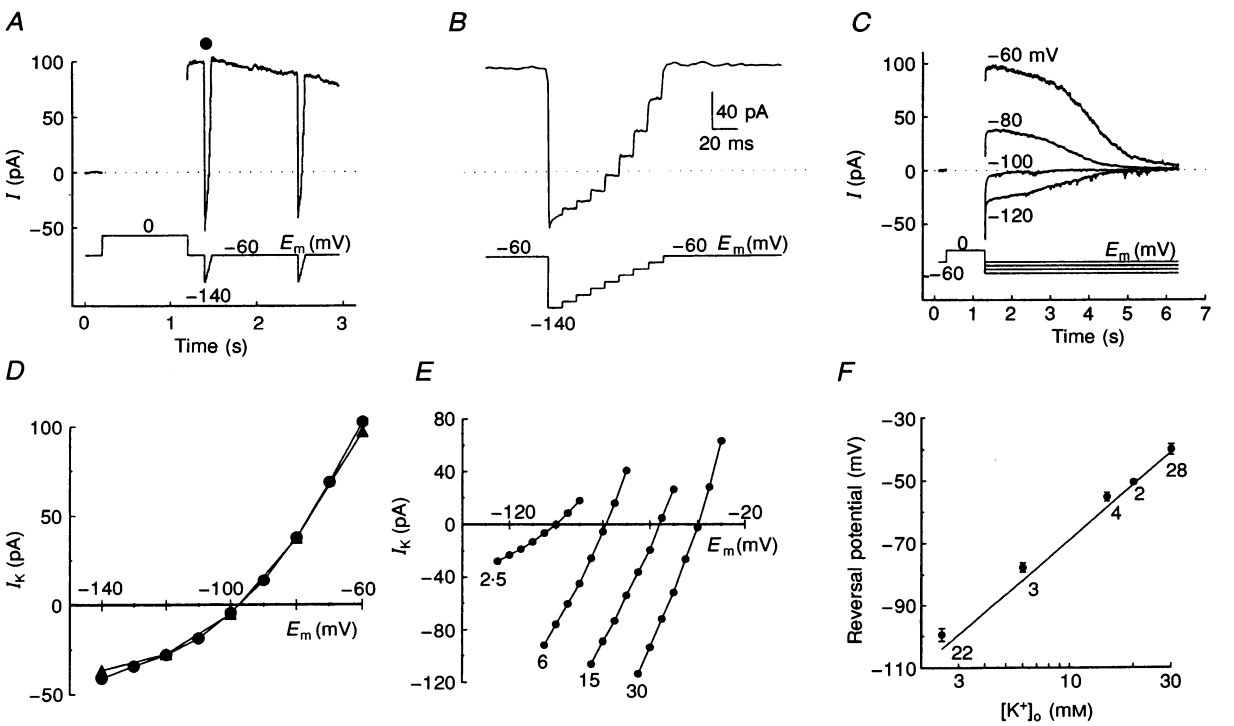

Figure 3. Measurement of reversal potential and K^+ selectivity of slow tail currents

A, a series of 10 ms voltage pulses from −140 to −60 mV in 10 mV steps was applied twice during repolarization (−60 mV), at 0·2 and 1·2 s after 1 s depolarization to 0 mV. $[K^+]_o = 2{\cdot}5$ mM, $[K^+]_i = 162$ mM. Cell capacitance, 3 pF. *B*, part marked by ● in *A* is shown on an expanded time scale. *C*, determination of tail-current reversal potential. The cell was stepped to 0 mV for 1 s from a holding potential of −60 mV, then returned to different repolarization potentials for 5 s. Recovery of 20 s was allowed between pulses. *D*, current–voltage relations from experiments in *A* (●) and *C* (▲). Both methods gave reversal potentials of −98 mV with 2·5 mM $[K^+]_o$. *E*, current–voltage relation when NaCl in normal Tyrode solution was replaced by equimolar KCl, using the protocol described in *A*. Values below the lines indicate the $[K^+]_o$ (mM). *F*, plot of reversal potential (means ± S.E.M.) against $[K^+]_o$. The numbers below data points indicate the number of cells. The continuous line is the predicted slope for a K^+-selective electrode at 22 °C: $E_K = (58{\cdot}6)\log([K^+]_o/[K^+]_i)$, where $[K^+]_i = 162$ mM.

of the tail current was sensitive to dTC block. The dashed line shows the expected dose–response relationship if 100% of the slow tail current were sensitive to dTC. The lower potency ($K_d = 20{\cdot}2$ μM) compared with apamin in 30 mM K^+ bath solution is associated with a quicker recovery from block (< 10 s) than is seen with apamin.

BK channels are reported to be sensitive to external TEA block ($K_d = 0{\cdot}2$–$0{\cdot}3$ mM) (Latorre *et al.* 1989; Solaro & Lingle, 1992), and SK channels less or not sensitive (Blatz & Magleby, 1986; Lang & Ritchie, 1990; Neely & Lingle, 1992*a*). The dose–response curve for external TEA block of the slow tail currents (Fig. 4*C*) gives a K_d of 5·4 mM at a holding potential of −60 mV with 2·5 mM K^+ in the bath solution, which is comparable with the K_d (3·1 mM) for TEA block of SK channels in the GH_3 cell line (Lang & Ritchie, 1990).

These pharmacological properties are consistent with the idea that slow tail currents in rat adrenal chromaffin cells mainly consist of K^+ currents through apamin-sensitive SK channels. However, high concentrations of apamin (~450 K_d) or dTC (~100 K_d) failed to block a fixed proportion (~8%) of slow tail currents. The dTC-resistant current has exactly the same time course as the apamin-resistant current ($n = 5$), implying both have similar Ca^{2+} sensitivity. Co-application of 2 μM apamin and 2 mM dTC did not increase the block further compared with that

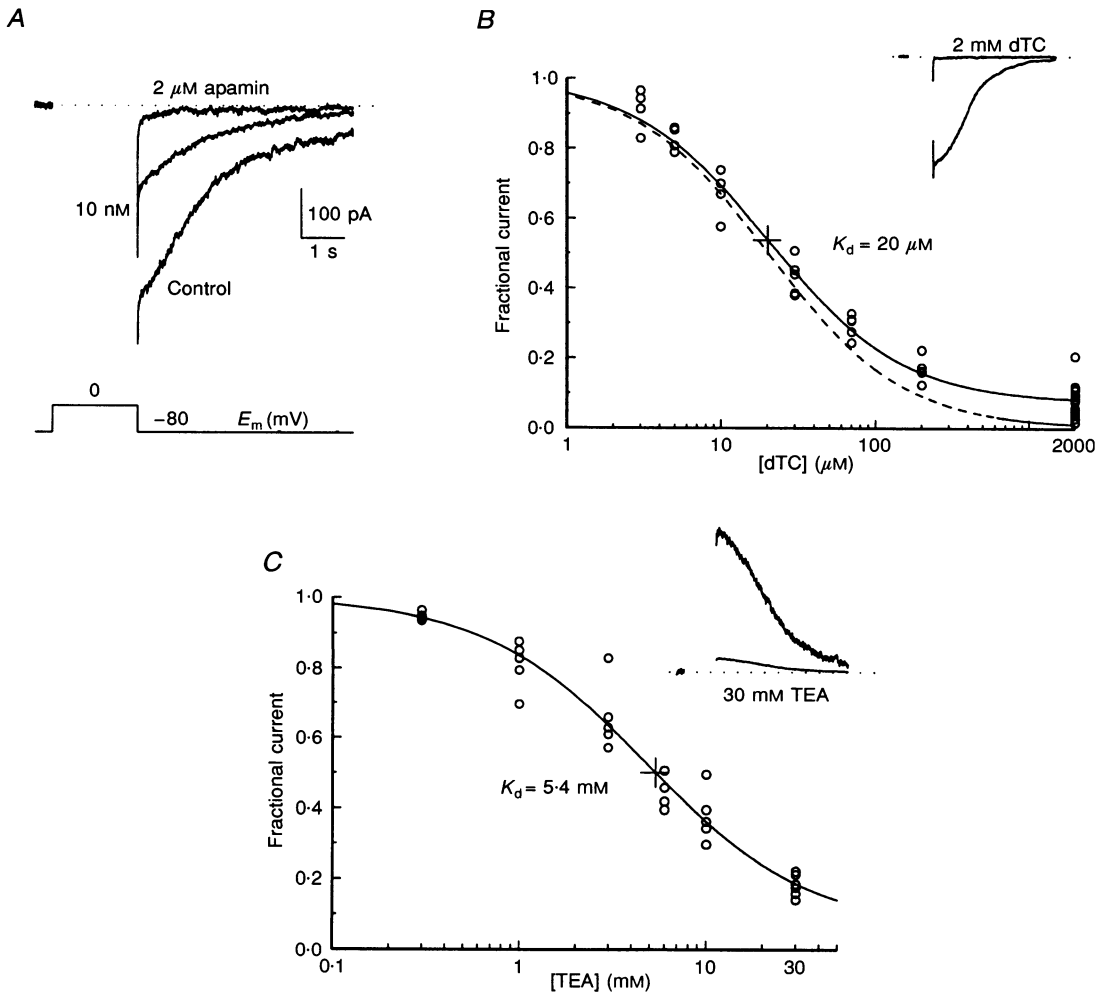

Figure 4. Pharmacological block of slow tail currents by apamin, *d*-tubocurarine (dTC) and TEA

A, effect of external apamin (10 nM and 2 μM) on slow tail current. In *A* and *B*, current traces were obtained in 30 mM K^+ Tyrode solution at a holding potential of −80 mV. *B*, dose–response curve for the external dTC block. $K_d = 20{\cdot}2$ μM. Note the incomplete block by 2 mM dTC (92 ± 5%, $n = 15$). The continuous line is a least-squares fit to the data for a 1:1 stoichiometry. The fit yields a maximum block of 93%. The dashed line represents the expected dose–response relation if 100% of the slow tail current were sensitive to dTC. Inset shows the effect of 2 mM dTC. *C*, dose–response curve for external TEA block. Currents were recorded with 2·5 mM K^+ Tyrode solution at −60 mV. $K_d = 5{\cdot}4$ mM. Inset shows the effect of 30 mM TEA. Note the reduction in current noise level with 30 mM TEA.

produced by 2 μM apamin alone (94·8 ± 2·6% with 2 μM apamin, and 95·1 ± 2·6% with 2 μM apamin and 2 mM dTC, $n = 4$), indicating that the apamin-resistant component represents the same population as the dTC-resistant one.

Other lines of evidence indicate that the apamin-resistant and apamin-sensitive components of slow tail current are from similar channels differing only in pharmacological characteristics. First, when the current in 2 μM apamin was scaled up, it had a time course similar to that without apamin or in 10 nM apamin ($n = 6$, data not shown). Second, addition of 5·4 mM TEA_o containing 2 μM apamin further reduced apamin-resistant tail current by approximately half (50 ± 7%, $n = 4$), indicating that apamin-resistant current has the same TEA sensitivity as the apamin-sensitive component. Third, the reversal potential of the apamin-resistant current was exactly the same as that of the slow tail current without apamin ($E_r = -41 \pm 1$ mV, $n = 4$).

Ion selectivity of the SK channel

Differentiation between monovalent cations by SK channels and the minimum pore diameter of the selectivity filter were investigated. Figure 5 shows current–voltage relations of whole-cell currents with 30 mM test cation and NMG as the major extracellular cations (for thallous ion, see Fig. 6*A*). NMG was practically impermeant in SK channels, giving no inward current even at −180 mV ($n = 3$; data not shown). The obviously permeant ions tested were Tl^+, Rb^+, Cs^+ and NH_4^+ (Figs 5*A* and *B*, and 6*A*). Ionic permeability, relative to that of K^+ (P_X/P_K), calculated from the average shift in reversal potential (eqn (1)) was: Tl^+ (1·87) > K^+ (1·0) > Rb^+ (0·81) > Cs^+ (0·16) > NH_4^+ (0·11) (Table 1). For Na^+ ($n = 5$) and Li^+ ($n = 8$), significant inward currents were not measured even at the membrane potential of −180 mV (Fig. 5*C*). Methylamine (MA) was tested to probe the pore size of the SK channel. No inward current was detected at −180 mV with MA ($n = 4$; Fig. 5*D*). Thus, it appears that SK channels are essentially impermeable to Na^+, Li^+ or MA ($P_X/P_K < 0{\cdot}005$, Table 1).

Relative conductance is another measure of ion selectivity. Measured as a zero-current slope conductance, the conductance ratio (g_X/g_K) was: Tl^+ (1·29) > K^+ (1·0) > Rb^+ (0·85) > Cs^+ (0·45) ≈ NH_4^+ (0·44) (Table 1). For Tl^+ and Rb^+, the conductance for inward current is not very different from the conductance for the outward K^+ current (Figs 5*B* and 6*A*), and conductance ratios are similar to permeability ratios (Table 1). The inward currents carried by Cs^+ and NH_4^+ were larger than

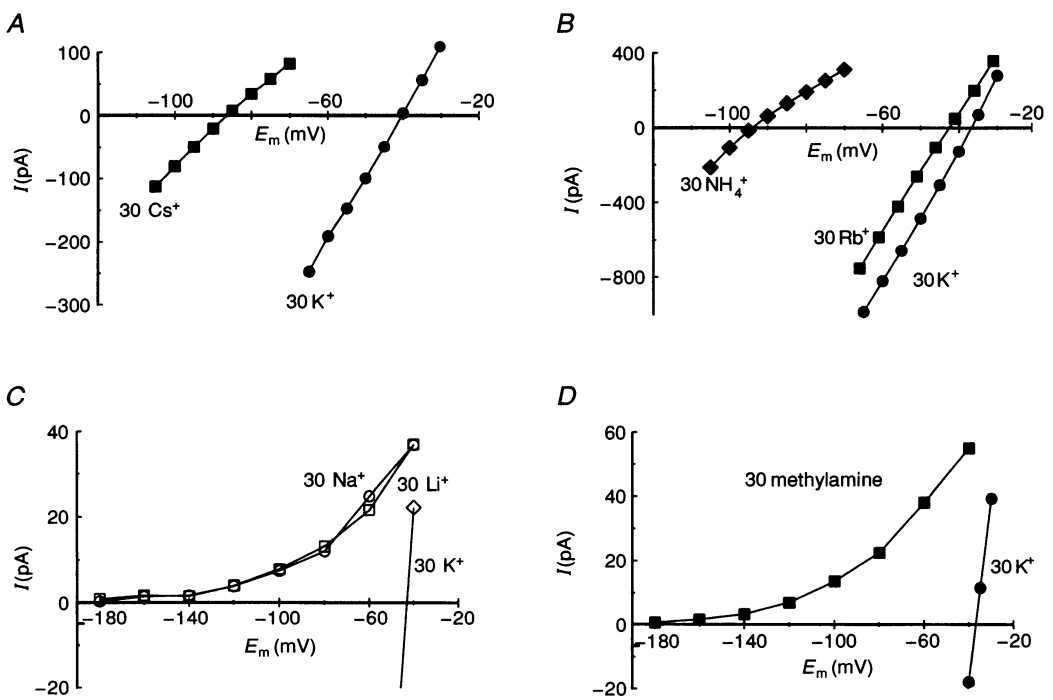

Figure 5. Measurement of reversal potential (E_r) under bi-ionic conditions using whole-cell recording

E_r was measured in bath solution containing 120 mM (NMG + MSA) and 30 mM test ion. $[K^+]_i = 162$ mM. *A*, Cs^+; *B*, Rb^+ and NH_4^+; *C*, Na^+ and Li^+; and *D*, methylamine. Note slight inward rectification with Cs^+ and NH_4^+. With Na^+, Li^+ or methylamine, no current reversal was observed even at −180 mV and SK channels ran down irreversibly, so outward currents became small, despite a large electrochemical gradient. In *C*, the line for K^+ connects points that are off the scale. All values in mM.

Table 1. Ion selectivity of the SK channel

Ion (X)	ΔE_r (mV)	P_X/P_K [a]	g_X/g_K [b]	Ion diameter [c] (nm)
Tl^+	16 ± 1·2 (4)	1·87	1·29	0·280
K^+	0	1·00	1·00	0·266
Rb^+	−5·4 ± 0·7 (17)	0·81	0·85	0·296
Cs^+	−47 ± 1·1 (9)	0·16	0·45	0·338
NH_4^+	−56 ± 1·7 (11)	0·11	0·44	0·320
Li^+	>−140 (8)	<0·005	—	0·120
Na^+	>−140 (5)	<0·005	—	0·190
MA	>−140 (4)	<0·005	—	0·378

The numbers in parentheses are the number of cells. [a] P (permeability) ratio is calculated using the Goldman–Hodgkin–Katz equation described in Methods. [b] g was measured as the zero-current slope conductance. Values of S.E.M. of g_X/g_K were 0·05 ($n = 4$), 0·06 ($n = 6$), 0·05 ($n = 6$) and 0·03 ($n = 4$) for Tl^+, Rb^+, Cs^+ and NH_4^+, respectively. [c] Ion diameter is the unhydrated ion diameter. Ion diameters of NH_4^+ and MA (methylamine) were measured from Corey–Pauling–Koltum (CPK) models.

expected on the basis of the permeability ratios and slight inward rectification was observed (Fig. 5*A* and *B*; Table 1). The Goldman–Hodgkin–Katz current equation, based on the independence principle (Hille, 1992), predicts outward-going rectification in this condition. These observations suggest that ions do not move independently in SK channels.

Slow tail currents ran down quite rapidly (several minutes) after replacement of external K^+ with impermeant ions. With the slow bath perfusion method, which took about 3–4 min for the measurement of a reversal potential for one kind of cation, slow tail currents measured in the presence of external K^+ decreased irreversibly to 10–50% of the initial amplitudes after a test of one impermeant cation, Na^+, Li^+, MA or NMG (Fig. 5*C* and *D*). A similar run-down was not observed with other permeant ions studied (Tl^+, Rb^+, Cs^+ and NH_4^+) and stable tail currents were recorded for as long as 1 h with external permeant ions.

Anomalous mole-fraction dependence

Mole-fraction behaviour, in which reversal potential or conductance is measured with varying mixtures of two different conducting ions, is a test of the conduction process (Hille & Schwarz, 1978). In a simple one-ion channel, in which at most one ion can occupy the conduction pathway and there are no additional allosteric

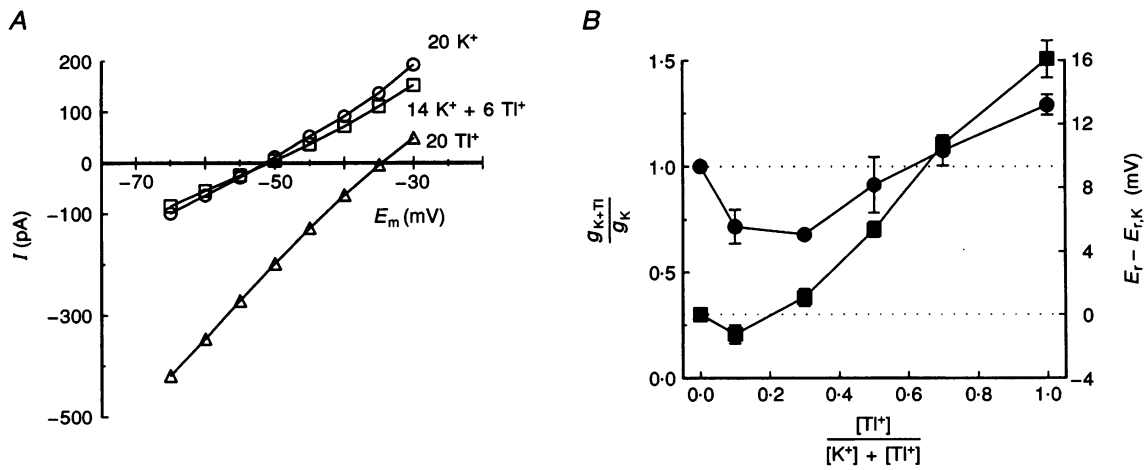

Figure 6. Anomalous mole-fraction dependence of zero-current slope conductance and reversal potential in mixtures of Tl^+ and K^+

$[Tl^+]_o + [K^+]_o = 20$ mM. $[K^+]_i = 162$ mM. *A*, current–voltage relations for (mM): 20 K^+ (○), 14 K^+ + 6 Tl^+ (□) and 20 Tl^+ (△). *B*, zero-current slope conductances (●) and reversal potential changes (■) plotted against the mole fraction of Tl^+ (4–5 measurements at each point). Conductance is normalized to that in 20 mM K^+. Major cation and anion were NMG and MSA. Standard error bars are smaller than symbols for some points.

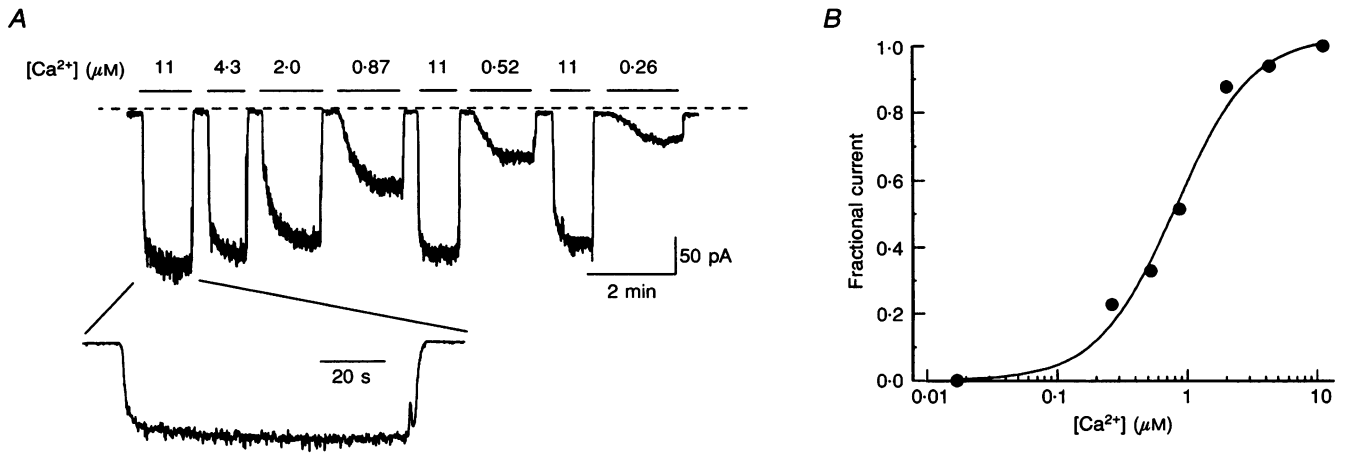

Figure 7. Ca^{2+} sensitivity of SK channels determined using inside-out macropatches
A, current trace obtained with alternating applications of 20 nM and various $[Ca^{2+}]_i$ solutions to the cytoplasmic side of the patch. Holding potential, −100 mV. Zero-current level is indicated by a dashed line. The inset shows response to 11 μM Ca_i^{2+} on an expanded time scale (×5). *B*, dose–response curve for Ca^{2+} activation of the steady-state current in the same patch. Data points are currents normalized to the steady-state current at 11 μM Ca_i^{2+}, which appeared to saturate the activation of $I_{K(Ca)}$ channels. A slight decrease of response to 11 μM Ca_i^{2+} with time (15% over 10 min) was compensated in the normalization process, assuming linear run-down of current with time. The Hill equation (continuous line) was fitted to the data using the least-squares method. $K_{½}$ = 0·80 μM, Hill coefficient = 1·46.

sites for ions, the membrane conductance or reversal potential in mixtures of ions A and B should be a monotonic function of the mole fraction:

$$[A]/([A]+[B]).$$

If the membrane conductance or reversal potential goes through a minimum or a maximum as a function of the mole fraction, then the channel is said to show anomalous mole-fraction dependence and might be a multi-ion pore (Hille & Schwarz, 1978). To examine the mole-fraction behaviour, reversal potentials and zero-current slope conductances were determined with extracellular solutions of varying mixtures of Tl^+ and K^+, maintaining the sum of $[Tl^+]_o$ and $[K^+]_o$ constant at 20 mM (Fig. 6). Even though Tl^+ ions carried greater currents through SK channels than K^+ (g_{Tl}/g_K = 1·29, Table 1) and were more permeant (P_{Tl}/P_K = 1·87, Table 1), there was a clear minimum in the zero-current slope conductance at mole

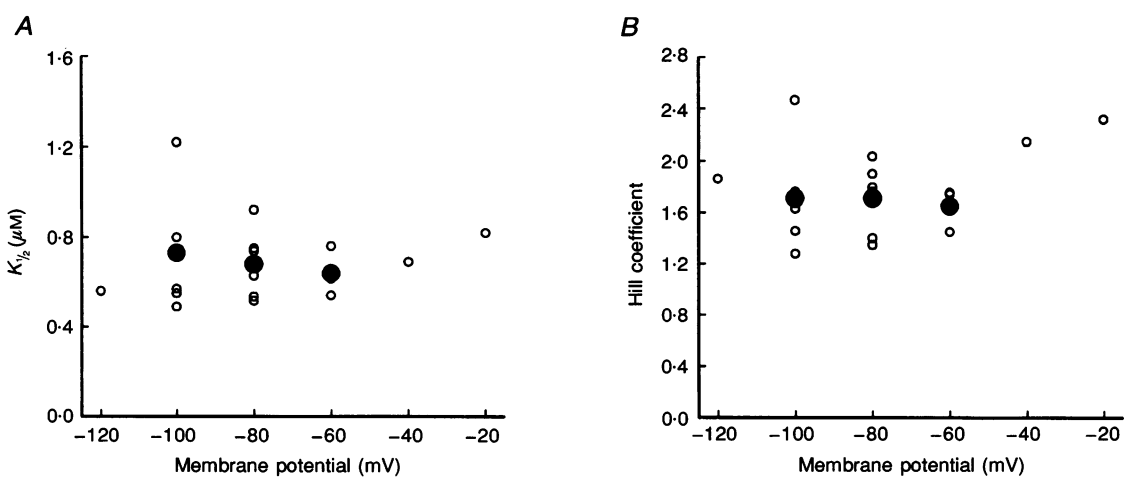

Figure 8. Lack of voltage sensitivity of SK channel gating
A, $K_{½}$ for Ca^{2+} activation against membrane potential. *B*, Hill coefficient against membrane potential. Individual data points (○) obtained from 8 macropatches are plotted together with their mean values (●).

fractions of Tl^+ between 0·1 and 0·3 ($n = 4$). The reversal potential behaviour was also non-monotonic, but the effect was not as large ($n = 5$). These results can be explained if the SK channel had multiple ion-binding sites with multiple ion occupancy.

Ca^{2+} and voltage sensitivity of the SK channel

The Ca^{2+} and voltage sensitivity of SK channels were determined by measuring Ca^{2+}-activated K^+ currents in inside-out macropatches. Figure 7*A* shows current traces for a patch perfused with different $[Ca^{2+}]_i$ values at a membrane potential of −100 mV. The time course of current rise depended on the $[Ca^{2+}]_i$. Raising $[Ca^{2+}]_i$ from 20 nM to 11 μM resulted in a rapid rise of inward current to ~250 pA (half-time of response ($t_{½}$) = 1·2 s), but the response to the solution with lower $[Ca^{2+}]_i$ was much slower (for example, $t_{½}$ = 14·6 s for 0·87 μM and 34 s for 0·26 μM). In contrast, the fall of current upon returning $[Ca^{2+}]_i$ to 20 nM was always relatively fast. It was faster when changing from 0·26 μM than from 11 μM ($t_{½}$ = 0·6 s for 0·26 μM and 2·1 s for 11 μM). The slow rise of current in response to increasing $[Ca^{2+}]_i$ might be caused by the diffusion delay due to the geometry of the Ω-shaped macropatch, withdrawn deep into the pipette tip, and the combined buffer capacity of EGTA (2 mM) and of endogenous Ca^{2+} buffers retained in excised patches (Neher & Augustine, 1992). When going from 20 nM to 11 μM Ca^{2+}, unbound EGTA in 20 nM Ca^{2+} solution and endogenous Ca^{2+} buffers inside the macropatch vesicle would buffer the influx of free Ca^{2+} through the narrow opening of the pipette tip and slow down the rise of free $[Ca^{2+}]_i$ inside the macropatch. In contrast, when decreasing $[Ca^{2+}]_i$ to 20 nM, the excess EGTA in the bath solution, mostly in unbound form, would bind free Ca^{2+} diffusing out of the vesicle solution and accelerate the decay of free $[Ca^{2+}]_i$ (Pallotta, Blatz & Magleby, 1992).

Fluctuation analysis of these macropatch currents showed that they are carried by channels of small conductance (5–11 pS, see next section). Occasional openings of BK channels were observed with 11 μM Ca^{2+} even at the membrane potential of −100 mV (see inset of Fig. 7*A*). The 20–30 pA spikes are consistent with currents through 275 pS BK channels in rat adrenal chromaffin cells (Solaro & Lingle, 1992). This BK channel activity is not likely to interfere with the measurement of Ca^{2+} sensitivity of SK channels since: the amplitude histogram of steady-state currents in response to 11 μM $[Ca^{2+}]_i$ followed a single Gaussian distribution (data not shown); opening frequency of BK channels was low even with 11 μM $[Ca^{2+}]_i$ at negative membrane potential; and current segments without spikes were chosen for measurement of steady-state current size.

The relative activation of SK channels in this experiment is plotted as a function of $[Ca^{2+}]_i$ in Fig. 7*B*. The observations are well fitted by a curve drawn according to the Hill equation, describing the co-operative binding of a ligand with a Hill coefficient of 1·46 and half-activation concentration ($K_{½}$) of 0·80 μM. In five experiments, the means ± S.E.M. of Hill coefficients and values of $K_{½}$ for Ca^{2+} activation at −100 mV were 1·71 ± 0·40 and 0·73 ± 0·27 μM, respectively.

Voltage sensitivity of SK channel gating by Ca^{2+} was examined by repeating the protocol of Fig. 7 at various holding potentials, ranging from −120 to −20 mV. Values of $K_{½}$ and Hill coefficients are plotted against membrane potentials in Fig. 8. The $K_{½}$ and Hill coefficient were 0·69 ± 0·18 μM ($n = 17$) and 1·70 ± 0·28 ($n = 17$), respectively, and neither had much voltage dependence. The small difference in $K_{½}$ was not statistically significant (ANOVA

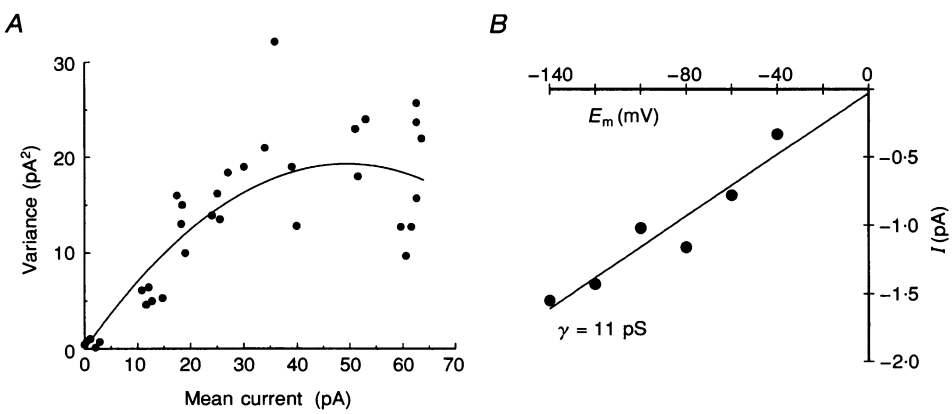

Figure 9. Fluctuation analysis of Ca^{2+}-activated macropatch current
A, plot of current variance *vs.* mean current at a holding potential of −60 mV. Fitting (see Methods) yielded a single channel current, i = 0·78 pA, and a number of channels, N = 127. *B*, plot of single-channel current *vs.* holding potential. Single-channel currents were estimated by repeating the fluctuation analysis described in *A* at other holding potentials. The slope of the least-squares linear fit was 11·3 pS and extrapolation gave a reversal potential of +2 mV. Slope conductance (γ) = 11 pS. The concentration of potassium aspartate was 160 mM on both sides of the membrane.

test, $P > 0{\cdot}05$). Hence the gating of SK channel has little voltage dependence over a potential range of −120 to −20 mV.

Single-channel conductance of the SK channel

Fluctuation analysis of macropatch current activated by Ca_i^{2+} was done to estimate single-channel conductance. At a membrane potential of −60 mV, unitary current amplitude estimated by fitting a parabola to the variance was 0·78 pA (Fig. 9*A*). The same analysis at other holding potentials gave the single-channel current–voltage relation (Fig. 9*B*). Least-squares linear fitting yielded a single-channel slope conductance of 11 pS and an extrapolated reversal potential of +2 mV. In two other patches, single-channel chord conductances were 5 and 6 pS (experiment of Fig. 7), assuming a reversal potential of 0 mV.

The single-channel current–voltage relation of SK channels was studied in inside-out patches. Rapid applications of 330 and 300 nM Ca^{2+} solution for 4–5 s at −80 mV activated four to five SK channels with unitary amplitude of 0·95 pA (Fig. 10*A*) and only one channel current level was observed with 260 nM Ca^{2+} solution. Figure 10*B* shows single-channel openings at various membrane potentials with 260 nM $[Ca^{2+}]_i$ in the same patch; records were chosen to illustrate discrete open and closed current levels rather than to be representative of the open probability, which is low at 260 nM Ca^{2+}. The current–voltage relation (Fig. 10*C*) was linear with a slope conductance (γ) of 14 pS and the extrapolated reversal potential was −8 mV with symmetrical (160 mM) K^+ as the major charge carrier (no Na^+ or Mg^{2+} on either side of the membrane). In another patch, the single-channel conductance was 13 pS. A detailed analysis of single-channel recording was not pursued due to the difficulty of isolating single-channel patches. Most patches contained quite a few SK channels even with the patch pipettes of ~20 MΩ.

DISCUSSION

This paper examines the ion selectivity and gating of apamin-sensitive SK channels in rat adrenal chromaffin cells. The SK channel has a permeability sequence similar to those of other K^+ channels ($Tl^+ > K^+ > Rb^+ > NH_4^+$), except that Cs^+ was quite permeant, suggesting a selectivity filter of 0·34–0·38 nm in diameter. The $K_{1/2}$ for the activation of SK channels by Ca_i^{2+} was ~0·7 μM, and the gating of SK channels shows little voltage dependence.

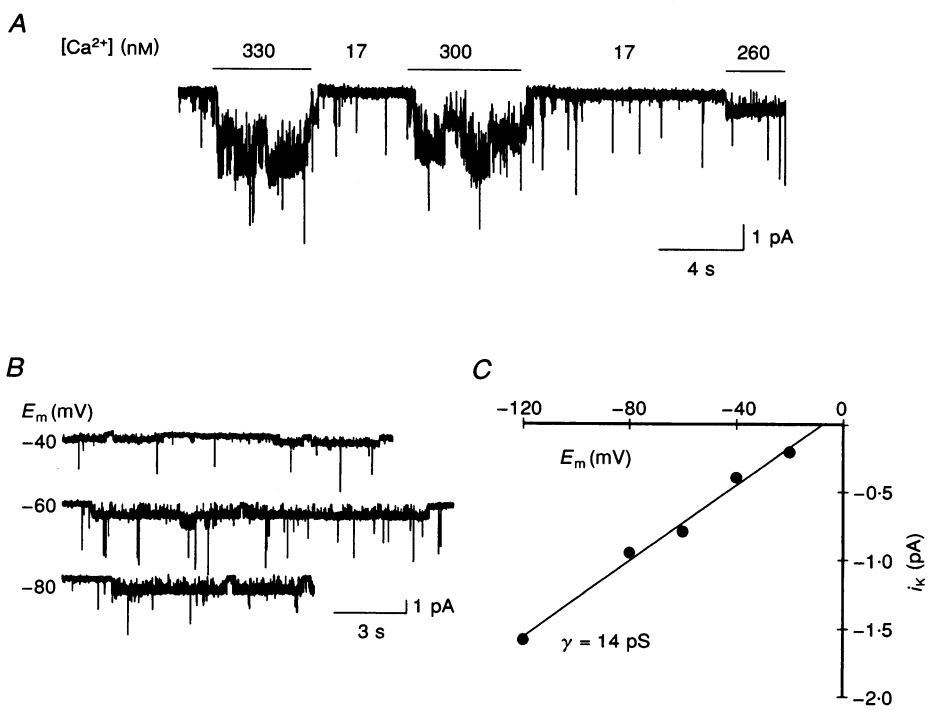

Figure 10. Single-channel recording of small-conductance Ca^{2+}-activated K^+ channels

A, SK channels were activated by rapid applications of high $[Ca^{2+}]_i$ solutions onto an inside-out patch. In addition, the patch contained a larger conductance K^+ channel (distinct from the BK channel) with very short openings that are not dependent on $[Ca^{2+}]_i$. Holding potential, −80 mV. Filter at 500 Hz, sampling at 1 kHz. *B*, sample single-channel recording at several holding potentials. $[Ca^{2+}]_i = 260$ nM. *C*, current–voltage relation of SK channels. Least-squares fitting gave a slope conductance of 13·9 pS and a reversal potential of −8 mV. The concentration of potassium aspartate was 160 mM on both sides of the membrane.

Isolation of SK currents as slow tail current

Intracellular Ca^{2+} is known to open non-selective cation, Cl^- and $I_{K(Ca)}$ channels (Marty, 1989). As described in Results, Ca^{2+}-activated Cl^- channels appear not to contribute to slow tail currents. Furthermore, slow tail currents were quite selective among alkali metal cations and Na^+ and Li^+ were not permeant (Fig. 5*C*; Table 1), excluding the possible contribution of Ca^{2+}-activated, non-selective cation channels to slow tail currents.

BK and SK channels have been reported in rat adrenal chromaffin cells (Neely & Lingle, 1992*a*). Pharmacological properties, Ca^{2+} sensitivity and voltage dependence of gating (see Results section) indicate that BK currents are not likely to contaminate the analysis of the slow tail currents. Slow tail currents were not blocked by 100 nM charybdotoxin (personal communication, C. Lingle at Washington University). Some portion of BK channels of rat chromaffin cells would become completely inactivated during the 1 s depolarization (Solaro & Lingle, 1992) and the remaining, non-inactivating BK currents would deactivate over the first 30 ms following repolarization (Neely & Lingle, 1992*a*).

The bi-exponential decay of slow tail currents activated by small Ca^{2+} entries (Figs 1*A* and 2*A*) may be explained by a simple model. The fast decay with $\tau = 100$–300 ms could be due to a rapid dissipation of steep, spatial gradients of $[Ca^{2+}]_i$ (Neher & Augustine, 1992) by diffusion from a submembrane domain at the site of Ca^{2+} entry. A simple calculation using Einstein's diffusion equation:

$$t = r^2/4D_{Ca},$$

where t represents time, r the mean diffusion distance and D_{Ca} the diffusion constant for Ca^{2+} (Hille, 1992), employing 6·6 μm for cell radius (calculated from the 5·4 pF capacitance of the cell in Fig. 2) and $0{\cdot}4 \times 10^{-6}$ cm^2 s^{-1} for D_{Ca} (Zhou & Neher, 1993), gives a time constant near 270 ms for spatial equilibration of $[Ca^{2+}]_i$. In bovine chromaffin cells which have similar dimensions, spatial gradients of $[Ca^{2+}]_i$ dissipate within 100–500 ms (Neher & Augustine, 1992). The decay-time constant of SK currents should be 1·7 times faster than that of $[Ca^{2+}]_i$ if the Hill coefficient for opening is ~1·7. The slow component with $\tau = 0{\cdot}8$–$1{\cdot}7$ s could be due to the slow uptake of Ca^{2+} into the intracellular stores and pumping out of the cell across the plasma membrane (Neher & Augustine, 1992).

The complex time course with plateau and slow decay phase following long depolarization may also be explained from the Ca^{2+} dependence of gating. The plateau may reflect the period when the falling $[Ca^{2+}]_i$ is still high enough to keep almost all SK channels open, and the later decay would then correspond to closure of channels as $[Ca^{2+}]_i$ returns towards resting levels. In bovine chromaffin cells, the time constant of exponential decay of elevated $[Ca^{2+}]_i$ is reported to be 7·2 s (Neher & Augustine, 1992). The much shorter time constant (1·4 s) of slow decay in this study may be due to differences in Ca^{2+} metabolism between the rat and bovine chromaffin cells or an acceleration of the decay phase due to the co-operativity of SK channel gating, which may be increased further in the presence of millimolar concentrations of Mg_i^{2+}, as in BK channels (Latorre *et al.* 1989).

Apamin block of slow tail current

Apamin has been used as a specific blocker of SK channels (Blatz & Magleby, 1987; Latorre *et al.* 1989). In some cells, it is considered to be a nearly irreversible blocker of SK channels (Goh & Pennefather, 1987; Grissmer, Lewis & Cahalan, 1992; Artalejo, García & Neher, 1993), though in others, e.g. hepatocytes (Cook & Haylett, 1985) and intestinal smooth muscle (Gater, Haylett & Jenkinson, 1985), the offset is more rapid. In rat chromaffin cells, the slow tail current was blocked by apamin with a K_d of 4·4 nM. At room temperature, the block reversed slowly ($\tau \approx 800$ s), which corresponds to an off-rate of $1{\cdot}3 \times 10^{-3}$ s^{-1}. From a K_d of 4·4 nM, the on-rate can be calculated as $2{\cdot}9 \times 10^5$ M^{-1} s^{-1}. These kinetic parameters are comparable to those obtained from rat brain synaptosomal membranes (Seagar *et al.* 1987), but the on-rate constant is orders of magnitude smaller than that reported for ^{125}I-labelled apamin binding to guinea-pig hepatocytes at 37 °C, where it approaches the diffusion-limited rate (Cook & Haylett, 1985).

Apamin- and dTC-insensitive component of slow tail current

Slow tail currents not blocked completely by apamin or dTC have been reported in several preparations (Goh & Pennefather, 1987; Ritchie, 1987; Neely & Lingle, 1992*a*; Artalejo *et al.* 1993). In rat chromaffin cells apamin- and dTC-insensitive $I_{K(Ca)}$ currents share several properties with apamin-sensitive SK currents, such as Ca^{2+} sensitivity, K^+ selectivity and TEA_o sensitivity.

These data suggest at least two possibilities. First, the apamin-insensitive current can represent a different population of $I_{K(Ca)}$ channels (for example, see Blatz & Magleby, 1986; Lang & Ritchie, 1990). Second, perhaps rat adrenal chromaffin cells have two variants of SK channels, with similar channel properties but different pharmacological properties. A minor variation in the amino acid sequence of the SK channel could bring about a big difference in the affinity for different blockers (for example, see MacKinnon & Yellen, 1990). The second hypothesis seems more likely because apamin-insensitive currents share many properties with apamin-sensitive currents. Yet another possibility, that binding of apamin or dTC leaves an 8% conductance in occupied SK channels, cannot be excluded.

Run-down of SK channels

SK channels were unstable in the absence of external permeant ions (Fig. 5*C* and *D*). In squid giant axon, the total absence of permeant ions on both sides of the membrane led to an irreversible loss of K^+ conductance (Almers & Armstrong, 1980). With SK channels and delayed rectifiers of mouse lymphocytes (Shapiro & DeCoursey, 1991), an irreversible run-down was observed in the absence of external permeant cations (albeit with high potassium internal solution). Interestingly, ^{125}I-labelled apamin binding to rat brain synaptic membranes was enhanced by external K^+ ions ($K_{½}$, 0·6 mM), and other alkali metal cations could be substituted for K^+ with an affinity sequence $Tl^+ = K^+ = Rb^+ > Cs^+ > NH_4^+ > Li^+$ or Na^+ (Seagar *et al.* 1987), which matches exactly with the permeability sequence of SK channels (Seagar *et al.* 1987; Table 1). It is suggested that cation binding to some intra-pore binding site(s), inaccessible from the intracellular side when the channel is closed, may stabilize a conformation of SK-channel protein that is important not only in determining the permeation property of SK channels but also for the binding of apamin at the outer mouth of the channel. Impermeant ions would not reach that binding site because of rejection at the selectivity filter or low affinity for the binding site. Similar modulation by $[K^+]_o$ has been observed in cloned voltage-gated K^+ channels, RCK4 (K_v1·4) and *Shaker* K^+ channels, where an amino acid that is important in the binding of external TEA is also important in determining K^+ dependence (López-Barneo, Hoshi, Heinemann & Aldrich, 1993).

Ion selectivity of SK channels

In this study, NH_4^+ and four alkali metal cations (Tl^+, K^+, Rb^+ and Cs^+) are measurably permeant in SK channels and these ions fall between 0·266 and 0·338 nm in unhydrated diameter (Table 1). In contrast, a slightly larger amine (MA) with a mean diameter of 0·378 nm was impermeant. These data suggest that the SK channel has a minimum pore diameter that lies between 0·34 and 0·38 nm. This is slightly larger than the suggested size of 0·30–0·33 nm for the delayed rectifier K^+ channel in frog myelinated nerve, which does not allow Cs^+ to pass (Bezanilla & Armstrong, 1972; Hille, 1973). However, a simple molecular sieving is not likely to be the only mechanism that determines the ion selectivity of SK channels since Li^+ and Na^+, which have much smaller unhydrated ion diameters than Cs^+, are impermeant. The equilibrium theory of ion selectivity by Eisenman (1962) demonstrated that only certain permeability sequences are predicted for alkali metal cations if selectivity is determined by a combination of specific binding and dehydration energies. The ion selectivity of SK channels follows Eisenman's sequence IV, which suggests ion binding site(s) of low electrostatic field strength. Na^+ and Li^+ might be excluded because they are more reluctant to lose their hydration water and are not adequately compensated for this loss by electrostatic and chemical interaction with the selectivity filter (Hille, 1992). In SK channels, it appears that both selection for the desired ions by specific binding and selection against undesired ions by rejection at a molecular sieve may contribute to determining the ion selectivity.

The SK channel is unique in that it is a selective K^+ channel in which Cs^+ is permeant and conducts large inward current (Table 1, Fig. 5*A*). Many K^+ channels, including the BK channel, are appreciably permeable to Tl^+, K^+, Rb^+ and NH_4^+ and not to Cs^+ (see Hille (1992) for review). Cs^+ permeability has been reported for a delayed rectifier and a transient A-type K^+ channel of *Helix* snail neurones (Reuter & Stevens, 1980; Taylor, 1987). These two channels differ from SK channels in that they are less selective among alkali metal cations, so Na^+ and Li^+ as well as Tl^+, Rb^+ and NH_4^+ are permeant. A similar permeability sequence for alkali metal cations has been described for a delayed rectifier K^+ channel in mouse lymphocytes (Shapiro & DeCoursey, 1991), a charybdotoxin-sensitive, 35 pS $I_{K(Ca)}$ channel of human T lymphocytes (Grissmer, Nguyen & Cahalan, 1993) and the cloned *Shaker* channel (Heginbotham & MacKinnon, 1993), but in all these channels, Cs^+ supports only small inward currents.

Gating of SK channels

The Hill coefficient gives an estimate of the minimum number of functional ligand-binding sites on a receptor and reflects the co-operativity of ligand binding onto the receptor. The apparent Hill coefficient for Ca^{2+} activation of SK channels is ~1·7 in this study (Fig. 8*B*), suggesting a requirement for at least two Ca^{2+}-binding sites. In rat superior cervical ganglion cells, a linear relationship between SK currents and $[Ca^{2+}]_i$ was observed in the absence of internal Mg^{2+} (Gurney, Tsien & Lester, 1987). In this study, however, $[Ca^{2+}]_i$ was not controlled directly. In contrast, apamin-sensitive SK channels of 4–7 pS in a human leukaemic T cell line have a Hill coefficient of 4–5 with 2 mM $[Mg^{2+}]_i$ (Grissmer *et al.* 1992). It would be interesting to pursue whether the Hill coefficient of SK channels in chromaffin cells is affected by $[Mg^{2+}]_i$.

The gating of SK channels shows little voltage dependence in terms of $K_{½}$ and the Hill coefficient (Fig. 8), which suggests that intrinsic voltage gating does not exist in SK channels and Ca^{2+} binding to the SK channel is voltage independent.

Physiological role of SK channels in rat chromaffin cells

In contrast to small SK currents in other cells (Ritchie, 1987; Artalejo *et al.* 1993), SK currents of rat chromaffin cells have been shown to make a large contribution to total outward currents during depolarizing pulses (Neely & Lingle, 1992*a*). Even though the relative activation of SK currents during action potentials of rat chromaffin cells

(Brandt, Hagiwara, Kidokoro & Miyazaki, 1976) and their contribution to the repolarization phase of action potential and after-hyperpolarization have not been studied quantitatively, existing data suggest that SK channels may be important in controlling the duration and frequency of action potentials and thereby the secretory activity of adrenal chromaffin cells. Single rat chromaffin cells fire spontaneous action potentials at rest (Brandt *et al.* 1976; Neely & Lingle, 1992*b*) and have spontaneous fluctuations of $[Ca^{2+}]_i$ from a resting level of 58 nM to 469 nM, possibly following action potentials (Malgaroli, Fesce & Meldolesi, 1990; Neely & Lingle, 1992*b*). Considering that $[Ca^{2+}]_i$ near the submembrane domain at the site of Ca^{2+} entry could be much higher than this (Neher & Augustine, 1992) and SK channels are activated around this $[Ca^{2+}]_i$ ($K_{½} \approx 0{\cdot}7$ μM), SK currents would be activated during action potentials, contributing to the repolarization phase of the action potential as well as to the after-hyperpolarization of rat chromaffin cells.

The high Ca^{2+} sensitivity of SK channels at negative membrane potentials suggests that SK channels would play important roles in modulating the secretion of chromaffin cells during periods of elevated $[Ca^{2+}]_i$. In cat adrenal chromaffin cells, muscarinic stimulation elevates $[Ca^{2+}]_i$ to ~1 μM and inhibition of SK channels by dTC or apamin increases the peak $[Ca^{2+}]_i$, prolongs the duration of $[Ca^{2+}]_i$ elevation and enhances catecholamine release evoked by muscarinic stimulation (Uceda, Artalejo, López, Abad, Neher & García, 1992). Comparable increases of $[Ca^{2+}]_i$ and activation of SK currents by muscarinic stimulation have been described in rat chromaffin cells (Neely & Lingle, 1992*b*). Activation of SK channels by elevated $[Ca^{2+}]_i$ would counteract the muscarinic depolarization, limiting the further firing of action potentials (see Tse & Hille, 1992). As in other cells, SK channels of rat chromaffin cells might act as a feedback mechanism that causes hyperpolarizing pauses between action potentials to modulate the frequency of action potentials and produce accommodation during sustained depolarization (Yarom *et al.* 1985; Lang & Ritchie, 1990; Hille, 1992).

REFERENCES

Almers, W. & Armstrong, C. M. (1980). Survival of K^+ permeability and gating currents in squid axons perfused with K^+-free media. *Journal of General Physiology* **75**, 61–78.

Artalejo, A. R., García, A. G. & Neher, E. (1993). Small-conductance Ca^{2+}-activated K^+ channels in bovine chromaffin cells. *Pflügers Archiv* **423**, 97–103.

Bezanilla, F. & Armstrong, C. M. (1972). Negative conductance caused by entry of sodium and cesium ions into the potassium channels of squid axons. *Journal of General Physiology* **60**, 588–608.

Blatz, A. L. & Magleby, K. L. (1986). Single apamin-blocked Ca-activated K^+ channels of small conductance in cultured rat skeletal muscle. *Nature* **323**, 718–720.

Blatz, A. L. & Magleby, K. L. (1987). Calcium-activated potassium channels. *Trends in Neurosciences* **10**, 463–467.

Brandt, B. L., Hagiwara, S., Kidokoro, Y. & Miyazaki, S. (1976). Action potentials in the rat chromaffin cell and effects of acetylcholine. *Journal of Physiology* **263**, 417–439.

Cook, N. S. & Haylett, D. G. (1985). Effects of apamin, quinine and neuromuscular blockers on calcium-activated potassium channels in guinea-pig hepatocytes. *Journal of Physiology* **358**, 373–394.

Eisenman, G. (1962). Cation selective glass electrodes and their mode of operation. *Biophysical Journal* **2**, suppl. 2, 259–323.

Gárdos, G. (1958). The function of calcium in the potassium permeability of human erythrocytes. *Biochimica et Biophysica Acta* **30**, 653–654.

Gater, P. R., Haylett, D. G. & Jenkinson, D. H. (1985). Neuromuscular blocking agents inhibit receptor-mediated increases in the potassium permeability of intestinal smooth muscle. *British Journal of Pharmacology* **86**, 861–868.

Goh, J. W. & Pennefather, P. S. (1987). Pharmacological and physiological properties of the after-hyperpolarization current of bullfrog ganglion neurones. *Journal of Physiology* **394**, 315–330.

Grissmer, S., Lewis, R. S. & Cahalan, M. D. (1992). Ca^{2+}-activated K^+ channels in human leukemic T cells. *Journal of General Physiology* **99**, 63–84.

Grissmer, S., Nguyen, A. N. & Cahalan, M. D. (1993). Calcium-activated potassium channels in resting and activated human T lymphocytes. *Journal of General Physiology* **102**, 601–630.

Gurney, A. M., Tsien, R. Y. & Lester, H. A. (1987). Activation of a potassium current by rapid photochemically generated step increases of intracellular calcium in rat sympathetic neurons. *Proceedings of the National Academy of Sciences of the USA* **84**, 3496–3500.

Hamill, O. P., Marty, A., Neher, E., Sakmann, B. & Sigworth, F. J. (1981). Improved patch-clamp techniques for high-resolution current recording from cells and cell-free membrane patches. *Pflügers Archiv* **391**, 85–100.

Heginbotham, L. & MacKinnon, R. (1993). Conduction properties of the cloned *Shaker* K^+ channel. *Biophysical Journal* **65**, 2089–2096.

Hille, B. (1973). Potassium channels in myelinated nerve: selective permeability to small cations. *Journal of General Physiology* **61**, 669–696.

Hille, B. (1992). *Ionic Channels of Excitable Membranes*, 2nd edn. Sinauer Associates, Inc., Sunderland, MA, USA.

Hille, B. & Schwarz, W. (1978). Potassium channels as multi-ion single-file pores. *Journal of General Physiology* **72**, 409–442.

Lang, D. G. & Ritchie, A. K. (1990). Tetraethylammonium blockade of apamin-sensitive and insensitive Ca^{2+}-activated K^+ channels in a pituitary cell line. *Journal of Physiology* **425**, 117–132.

Latorre, R., Oberhauser, A., Labarca, P. & Alvarez, O. (1989). Varieties of calcium-activated potassium channels. *Annual Review of Physiology* **51**, 385–389.

López-Barneo, J., Hoshi, T., Heinemann, S. H. & Aldrich, R. W. (1992). Effects of external cations and mutations in the pore region on C-type inactivation of *Shaker* potassium channels. *Receptors and Channels* **1**, 61–71.

MacKinnon, R. & Yellen, G. (1990). Mutations affecting TEA blockade and ion permeation in voltage-activated K^+ channels. *Science* **250**, 276–279.

Malgaroli, A., Fesce, R. & Meldolesi, J. (1990). Spontaneous $[Ca^{2+}]_i$ fluctuations in rat chromaffin cells do not require inositol 1,4,5-trisphosphate elevations but are generated by a caffeine- and ryanodine-sensitive intracellular Ca^{2+} store. *Journal of Biological Chemistry* **265**, 3005–3008.

Martell, A. & Smith, R. M. (1974). *Critical Stability Constants*, vol. I & II. Plenum, New York.

MARTY, A. (1981). Ca-dependent K channels with large unitary conductance in chromaffin cell membranes. *Nature* **291**, 497–500.

MARTY, A. (1989). The physiological role of calcium dependent channels. *Trends in Neurosciences* **11**, 420–424.

NEELY, A. & LINGLE, C. J. (1992*a*). Two components of calcium-activated potassium current in rat adrenal chromaffin cells. *Journal of Physiology* **453**, 97–131.

NEELY, A. & LINGLE, C. J. (1992*b*). Effects of muscarine on single rat adrenal chromaffin cells. *Journal of Physiology* **453**, 133–166.

NEHER, E. & AUGUSTINE, G. J. (1992). Calcium gradients and buffers in bovine chromaffin cells. *Journal of Physiology* **450**, 273–301.

PALLOTTA, B. S., BLATZ, A. L. & MAGLEBY, K. L. (1992). Recording from calcium-activated potassium channels. In *Methods in Enzymology*, vol. 207, *Ion Channels*, ed. RUDY, B. & IVERSON, L. E., pp. 194–207. Academic Press, San Diego, CA, USA.

PARK, Y. B. & HILLE, B. (1993). Gating and selectivity of apamin-sensitive, Ca-activated K channels of small conductance in rat adrenal chromaffin cells. *Society for Neuroscience Abstracts* **19**, 550.2.

REUTER, H. & STEVENS, C. F. (1980). Ion conductance and ion selectivity of potassium channels in snail neurones. *Journal of Membrane Biology* **57**, 103–118.

RITCHIE, A. K. (1987). Two distinct calcium-activated potassium currents in a rat anterior pituitary cell line. *Journal of Physiology* **385**, 591–609.

SEAGAR, M. J., MARQUEZE, B. & COURAUD, F. (1987). Solubilization of the apamin receptor associated with a calcium-activated potassium channel from rat brain. *Journal of Neuroscience* **7**, 565–570.

SHAPIRO, M. S. & DECOURSEY, T. E. (1991). Selectivity and gating of the type *l* potassium channel in mouse lymphocytes. *Journal of General Physiology* **97**, 1227–1250.

SIGWORTH, F. J. (1980). The variance of sodium current fluctuations at the node of Ranvier. *Journal of Physiology* **307**, 97–129.

SOLARO, C. R. & LINGLE, C. J. (1992). Trypsin-sensitive, rapid inactivation of a calcium-activated potassium channel. *Science* **257**, 1694–1698.

TAYLOR, P. S. (1987). Selectivity and patch measurements of A-current channels in *Helix aspersa* neurones. *Journal of Physiology* **388**, 437–447.

TSE, A. & HILLE, B. (1992). GnRH-induced Ca^{2+} oscillations and rhythmic hyperpolarizations of pituitary gonadotropes. *Science* **255**, 462–464.

UCEDA, G., ARTALEJO, A. R., LÓPEZ, M. G., ABAD, F., NEHER, E. & GARCÍA, A. G. (1992). Ca^{2+}-activated K^+ channels modulate muscarinic secretion in cat chromaffin cells. *Journal of Physiology* **454**, 213–230.

YAROM, Y., SUGIMORI, M. & LLINÁS, R. (1985). Ionic currents and firing patterns of mammalian vagal motoneurons *in vitro*. *Neuroscience* **16**, 719–737.

ZHOU, Z. & NEHER, E. (1993). Mobile and immobile calcium buffers in bovine adrenal chromaffin cells. *Journal of Physiology* **469**, 245–273.

Acknowledgements

I am most grateful to Dr B. Hille for letting me work in his laboratory, for financial support and invaluable discussions throughout the various stages of this study. I would like to thank Dr J. Herrington for introducing me to rat adrenal chromaffin cells for this study and the rapid perfusion system. I also thank Drs A. Golard, J. Herrington, J. Kirillova, K. Mackie, M. S. Shapiro and L. P. Wollmuth, for helpful discussion and comments on the manuscript and L. Miller and D. Anderson for technical assistance. This work was supported by grant NS08174 from the National Institutes of Health and by awards from the McKnight and W. M. Keck Foundations.

Received 8 February 1994; accepted 13 May 1994.